Title

Adaptive Evolution of Thermotoga maritima Reveals Plasticity of the ABC Transporter Network

Journal

Applied and Environmental Microbiology, 81(16)

ISSN

0099-2240

Authors

Latif, Haythem
Sahin, Merve
Tarasova, Janna
et al.

Publication Date

2015-08-15

DOI

10.1128/aem.01365-15

Peer reviewed

AEM
Journals.ASM.org

Adaptive Evolution of *Thermotoga maritima* Reveals Plasticity of the ABC Transporter Network

Haythem Latif, Merve Sahin, Janna Tarasova, Yekaterina Tarasova, Vasiliy A. Portnoy, Juan Nogales,* Karsten Zengler

Department of Bioengineering, University of California, San Diego, La Jolla, California, USA

Thermotoga maritima **is a hyperthermophilic anaerobe that utilizes a vast network of ABC transporters to efficiently metabolize a variety of carbon sources to produce hydrogen. For unknown reasons, this organism does not metabolize glucose as readily as it does glucose di- and polysaccharides. The leading hypothesis implicates the thermolability of glucose at the physiological temperatures at which *T. maritima* lives. After a 25-day laboratory evolution, phenotypes were observed with growth rates up to 1.4 times higher than and glucose utilization rates exceeding 50% those of the wild type. Genome resequencing revealed mutations in evolved cultures related to glucose-responsive ABC transporters. The native glucose ABC transporter, GluEFK, has more abundant transcripts either as a result of gene duplication-amplification or through mutations to the operator sequence regulating this operon. Conversely, BglEFGKL, a transporter of beta-glucosides, is substantially downregulated due to a nonsense mutation to the solute binding protein or due to a deletion of the upstream promoter. Analysis of the ABC2 uptake porter families for carbohydrate and peptide transport revealed that the solute binding protein, often among the transcripts detected at the highest levels, is predominantly downregulated in the evolved cultures, while the membrane-spanning domain and nucleotide binding components are less varied. Similar trends were observed in evolved strains grown on glycerol, a substrate that is not dependent on ABC transporters. Therefore, improved growth on glucose is achieved through mutations favoring GluEFK expression over BglEFGKL, and in lieu of carbon catabolite repression, the ABC transporter network is modulated to achieve improved growth fitness.**

Cells are continually changing and adapting in an effort to find an optimal state given the environmental conditions they encounter (1–4). The dynamic nature of regulatory networks (5–8) and the evolution of genomes in response to prolonged exposure to a given environment (4) are manifested in changes in the cell's phenotype. Thus, the genotype, the phenotype, and the environment that the microbes inhabit are intricately connected (1–4, 9, 10). A fundamental step in understanding the behavior of living systems is to reveal the connections underpinning the genotype-phenotype relationship. Between the genotype and phenotype lie many cellular processes such as transcription, translation, RNA degradation, and protein turnover, all of which are governed by complex regulatory networks.

An approach to better define the genotype-phenotype relationship is to track evolutionary changes in a laboratory setting (11–13). Laboratory evolution is a systematic approach to examine the dynamic response cells that undergo when the environmental state is changed. Prolonged exposure to a perturbed environment such as elevated growth temperatures (14, 15) or exposure to a nonnative carbon source (16) may result in adapted regulation and/or genetic changes that result in improved phenotypic properties. Throughout the laboratory evolution, physiological properties are measured and related back to the original phenotype. This can then be coupled with multiple genome-scale approaches to identify the underlying changes that produced the new phenotype (12, 13). Integrated analysis of genome resequencing data and gene expression profiling has been demonstrated to reveal causal mutations and the downstream impact of those on regulation, transcription, and protein functionality (11–13). The simplicity of laboratory evolution experiments and the advent of next-generation sequencing makes any culturable microorganism a candidate for an evolution study, providing insight into the different mechanisms underlying adaptation and evolution.

Here, laboratory evolution was applied to study the genotype-phenotype relationship in *Thermotoga maritima*. *T. maritima* is the best-characterized species of the *Thermotogae* phylum. *Thermotogae* are found at the base of the bacterial 16S rRNA gene-based phylogenetic tree (17, 18). Although the exact depth of the phylum has been a matter of debate (19, 20), the phylum is consistently considered deep branching and, as such, has been the focus of several evolutionary studies (19, 21–26). Furthermore, organisms from hydrothermal vent communities, such as *T. maritima*, are thought to harbor traits of early life (27). *T. maritima* grows anaerobically and has an optimal growth temperature of 80°C (28). The microorganism is strictly fermentative and capable of converting a large variety of mono-, di-, and polysaccharides to produce hydrogen with high stoichiometric efficiency. As a source of thermostable enzymes and as an efficient producer of hydrogen, *T. maritima* has garnered interest for many biotechnology applications (29, 30).

Received 27 April 2015 **Accepted** 28 May 2015

Accepted manuscript posted online 5 June 2015

Citation Latif H, Sahin M, Tarasova J, Tarasova Y, Portnoy VA, Nogales J, Zengler K. 2015. Adaptive evolution of *Thermotoga maritima* reveals plasticity of the ABC transporter network. Appl Environ Microbiol 81:5477–5485. doi:10.1128/AEM.01365-15.

Editor: M. Kivisaar

Address correspondence to Karsten Zengler, kzengler@ucsd.edu.

* Present address: Juan Nogales, Department of Environmental Biology, Centro de Investigaciones Biológicas-CSIC, Madrid, Spain.

Supplemental material for this article may be found at http://dx.doi.org/10.1128/AEM.01365-15.

doi:10.1128/AEM.01365-15

The genome sequence of *T. maritima* was first completed in 1999 and revealed that *T. maritima* has no phosphotransferase system and is heavily reliant on ATP binding cassette transporters (ABC transporters) for the import of carbon sources (20). Recently, this genome has been updated to include a 10-kb gap that was missing in the initial assembly (31, 32). This cassette encodes two ABC transporters primarily responsible for the transport of glucose (*gluEFK*) and trehalose (*treEFG*) (32–34). ABC transport genes account for nearly 60% of all classified transporter proteins in this organism and for nearly 10% of all protein-coding genes. Of the 173 ABC transporters found in *T. maritima*, 139 belong to the ABC2 uptake family. It is this vast network of ABC transporters that enables *T. maritima* to metabolize such a diverse set of carbon sources. However, growth on di- and polysaccharides, such as maltose and starch, is typically faster than that on monosaccharides (34). The average doubling time for *T. maritima* grown on glucose, mannose, and xylose was found to be more than double that for growth on various polysaccharides (200 min and 90 min, respectively) (35). It has been suggested that glucose is not readily metabolized due to its thermolability at the physiological growth temperature of *T. maritima* (29). No carbon catabolite repression system is known to exist in *T. maritima* (34–36), and the bacterium is known to metabolize multiple carbon sources simultaneously (36).

Recent advances in genome characterization of *T. maritima* have significantly enhanced our understanding of regulation and gene expression in this microorganism. A comprehensive and detailed reconstruction of the carbohydrate utilization regulatory network revealed that each of the 17 local transcription factor regulons controls at most seven operons (33, 34). Most of the *T. maritima* ABC2 uptake transporters are controlled via transcription factors in this network. Complementary to these efforts, the transcription start sites, transcription units, and σ^{70} promoter composition were defined for *T. maritima* in a multiomic data integration effort (31).

Here, the genotype-phenotype relationship in *T. maritima* was studied through a multiomic, genome-scale characterization of laboratory-evolved cultures grown with glucose as the sole carbon source. Wild-type cultures were continually passaged until no additional growth improvements were observed. These cultures were then characterized physiologically, genetically, and through gene expression profiling, and the results were analyzed in comparison with those for the wild-type strain. In doing so, the inherent growth limitations for *T. maritima* growing on glucose were revealed and the underlying genetic modifications and regulatory changes that alleviate this limitation were interrogated.

MATERIALS AND METHODS

Culture conditions and physiology. *Thermotoga maritima* MSB8 ATCC cultures were grown anaerobically at 80°C in chemically defined minimal medium (see Table S1 in the supplemental material) (37). For glucose laboratory evolution, cultures were serially passaged on 10 mM glucose in 120-ml serum bottles with 50-ml working volumes daily. Cultures were passaged using variable inoculum volumes to ensure that cells were kept between the mid- and late-exponential phases. Inoculum volume was determined by using the calculated growth rate, which was found through an exponential curve fit between the target starting and harvest measurements of optical density at 600 nm (OD_{600}) as a function of time. Evolutions were terminated upon observation of a plateau in the calculated growth rate. Glycerol adaptation was performed under similar growth conditions (0.5% [wt/vol] final concentration) by an initially prolonged incubation (2 to 3 weeks) until growth was detected using OD_{600}. The adaptation was continued for an additional month with the time between passages decreasing. The physiology of evolved cultures was assessed using a batch bioreactor setup with continuous N_2/CO_2 gas sparging and pH control set to 6.5 as previously described (31). Growth in the bioreactors was assessed using OD_{600} measurements. Simultaneously, samples were collected for extracellular glucose and acetate measurements using high-pressure liquid chromatography (HPLC) (Aminex HPX-87H column number 125-0140). Cells were collected during exponential phase for total RNA isolation and, subsequently, gene expression studies via transcriptome sequencing (RNA-seq).

Genomic DNA sequencing and variant analysis. Genomic DNA was isolated from evolved cultures using standard phenol-chloroform-isoamyl alcohol extraction techniques. Sequencing libraries were constructed using a Nextera XT DNA sample preparation kit (Illumina) following the vendor's instructions. Paired-end libraries were then sequenced (2×250) on an Illumina MiSeq platform. Genetic variants were detected using the Breseq software package (4) with the NC_021214 reference genome sequence and annotation. This reference genome was constructed using Illumina paired-end reads. The raw reads used to assemble this genome (SRX233319) were also analyzed using Breseq to exclude potential assembly errors from variant analysis. The Breseq flags for copy number variation and polymorphism prediction were turned on. Mutations with a frequency exceeding 30% were considered significant in this study.

RNA-seq and transcript abundance estimation. Total RNA was isolated from exponentially growing cells harvested during bioreactor experiments. Biological replicates of each mutant were enzymatically lysed as previously described (31). Crude lysate was then purified for total RNA using the RNeasy minikit (Qiagen) with on-column DNase treatment. Total RNA was quantified using a NanoDrop (Thermo Scientific), and the quality was checked using a Bioanalyzer (Agilent). Purified total RNA was then prepared for Illumina sequencing as previously described (31). Paired-end, strand-specific RNA-seq was performed using the dUTP method (38). rRNA was depleted using the Ribo-Zero rRNA removal kit for bacteria (Epicentre). rRNA-depleted RNA was then fragmented using Ambion's RNA fragmentation reagent. Reverse transcription was primed using random hexamers. Completed libraries were sequenced using the Illumina MiSeq platform. Paired-end reads were mapped against the NC_021214 genome using bowtie2 with default settings (39). Subsequent alignment files were processed using Cuffdiff from the Cufflinks suite of tools for determination and comparative analysis of fragments per kilobase of transcript per million fragments mapped (or FPKMs as defined in Cufflinks) (40).

Gene expression analysis. Regulon information on *T. maritima* was obtained from Regpricise (41) and from publications defining the sugar regulons in *T. maritima* (33, 34). Hypergeometric enrichment was performed using the scipy function "hypergeom." Heat maps were generated using the R package "gplots" function heatmap.2. Clusters of orthologous groups (COGs) were extracted from the Integrated Microbial Genomes (IMG) database (42). Genes belonging to the Transporter Classification Database (TCDB) (43) ABC transporter superfamily (3.A.1) were identified in IMG. Family predictions were performed using TransporterTP (44). TCDB families belonging to the ABC2 uptake family were defined by Zheng et al. (45). RNAFold from the ViennaRNA Package (46) was used for prediction of hairpin structures using default settings and a temperature set point of 80°C.

Genome-scale metabolic modeling. The genome-scale model of *T. maritima* iTZ479_v2 (47) was used for predicting flux distributions. To construct condition-specific metabolic models, the glucose uptake rate and acetate production rate of each strain (Table 1) were used in iTZ479_v2 as additional constraints. Additionally, since lactate and alanine were not detected in the supernatant, the fluxes through the corresponding exchange reactions were constrained to zero. The distributions of feasible fluxes in the condition-specific models were calculated using

TABLE 1 Physiological properties of glucose-evolved cultures[a]

Culture	Growth rate (1/h)	Doubling time (h)	Relative fitness	Glucose utilization rate [mmol/(g dry cell wt · h)]	Acetate production rate [mmol/(g dry cell wt · h)]	Acetate/glucose ratio
TM-wt	0.095 ± 0.027	7.8 ± 2.6	1.00	6.1 ± 1.5	10.1 ± 2.9	1.7 ± 0.11
eTMglc1	0.230 ± 0.036	3.1 ± 0.5	2.43	9.6 ± 1.5	12.5 ± 2.3	1.3 ± 0.05
eTMglc2	0.151 ± 0.004	4.6 ± 0.1	1.60	8.6 ± 1.7	11.7 ± 2.3	1.4 ± 0.11
eTMglc3	0.214 ± 0.004	3.2 ± 0.1	2.26	7.7 ± 1.7	10.2 ± 2.3	1.3 ± 0.11

[a] Values are means ± standard deviations.

Markov chain Monte Carlo sampling (48). The feasible flux distribution was obtained using an artificially centered hit-and-run algorithm as previously described (49). For the wild type, eTMglc1, eTMglc2, and eTMglc3 models, mixed fractions of 0.48, 0.49, 0.50, and 0.49 were obtained, respectively, indicating that the solution space for each condition-specific model was uniformly sampled. All computational simulations were performed using the COBRA toolbox (50) in the MATLAB environment. Linear optimization problems were solved using the GNU linear programming kit (GLPK) (http://www.gnu.org/software/glpk).

Microarray data accession number. Data are publically available through the Gene Expression Omnibus under series GSE63141.

RESULTS

Glucose evolution and evolved phenotypic properties. Glucose evolution was conducted under batch conditions with daily serial passaging. Cultures were maintained in exponential phase using a variable seed inoculum calculated from calculated growth rates. Figure 1 shows the increase in calculated growth rate for the three evolved cultures generated in this study and the number of generations needed to achieve these endpoints. The evolution was completed within 25 days and 240 generations. Beyond 15 days (120 generations), no observed improvements in calculated growth rates were observed. The evolutionary endpoints generated here have a cumulative number of cell divisions (CCD) of 4.3×10^9 to 6.0×10^9, which is three orders of magnitude lower than that observed for *Escherichia coli* evolution experiments (51).

Further characterization of the phenotypic properties of the evolved cultures was conducted using a series of batch bioreactor experiments where the pH was maintained at a set point of 6.5 and the accumulation of inhibitory levels of hydrogen was prevented by implementing a continuous gassing strategy with an 80:20 N_2-CO_2 mix. Triplicate biological replicates for the three evolved cultures and the wild type (TM-wt) were grown on 10 mM glucose in bioreactors. The designations eTMglc1, eTMglc2, and eTMglc3 are used to reference the evolved culture. Growth rates, glucose uptake rates, acetate production rates, and other physiological metrics are presented in Table 1. All three strains showed improved growth on glucose with relative fitness improvements ranging from 60 to 143%. They also showed improved glucose utilization rates (26 to 57%), while the acetate production rates did not significantly change. Therefore, the improved growth fitness does not maintain the same efficiency of conversion of glucose to acetate as for the wild type. Other than acetate, no other organic metabolic products were found in detectible quantities. *In silico* predictions using a genome-scale model of *T. maritima* metabolism were applied to reconcile the loss of acetate conversion efficiency observed in the evolved strains. Using the physiological data generated for Table 1 and the lack of observed organic products (other than acetate), strain-specific simulations were conducted. The carbon flux predictions suggested that the higher glucose influx observed in the evolved strains overflowed, at some extent, the glycolytic pathway, and as a consequence, a significant amount of glucose-6-phosphate was funneled through the oxidative branch of the pentose phosphate pathway. This metabolic rerouting is compatible with the lower acetate/glucose ratio found in the evolved strains compared with the wild type and supports greater yields of carbon dioxide in the evolved strains, thus closing the carbon mass-balance (see Fig. S1 in the supplemental material).

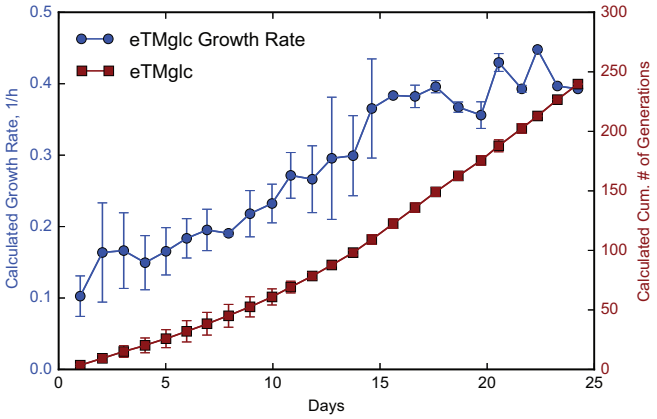

FIG 1 Glucose evolution time course. This plot shows the calculated growth rate (blue) and cumulative number of generations (red) needed to achieve the evolved phenotype for *T. maritima* grown on glucose as the sole carbon source. Traces represent the average of calculated values across all the three cultures, and the error bars represent ±1 standard deviation across the evolved replicates. Evolutionary endpoints were determined at 25 days and 250 generations due on an observed plateau in the calculated growth rate.

Genetic variants in evolved cultures on glucose. The evolved cultures (eTMglc) were sequenced to determine possible causal mutations for the observed growth phenotype. Genomic DNA was isolated and sequenced on an Illumina MiSeq with the mean fit coverage exceeding 250× for all cultures. Genetic variants were detected using the Breseq software package. Table S2 in the supplemental material summarizes the genetic variants detected. A total of 21 mutations were present in at least one of the replicates. Of the 14 unique gene products associated with mutations, 9 are membrane-associated/membrane-spanning proteins. ABC transporter genes, their associated transcription factor, or the intergenic region upstream of ABC transporter genes represents 6 of the 14 unique mutations. One mutation was shared across all evolved cultures, which occurs in the transfer-messenger RNA (tmRNA) gene (Tmari_R0031) at position 195, deleting a G within a G stretch that is predicted to form the last Watson-Crick base pair at the 3′ end of pseudoknot 3 by tmRDB (52). Therefore,

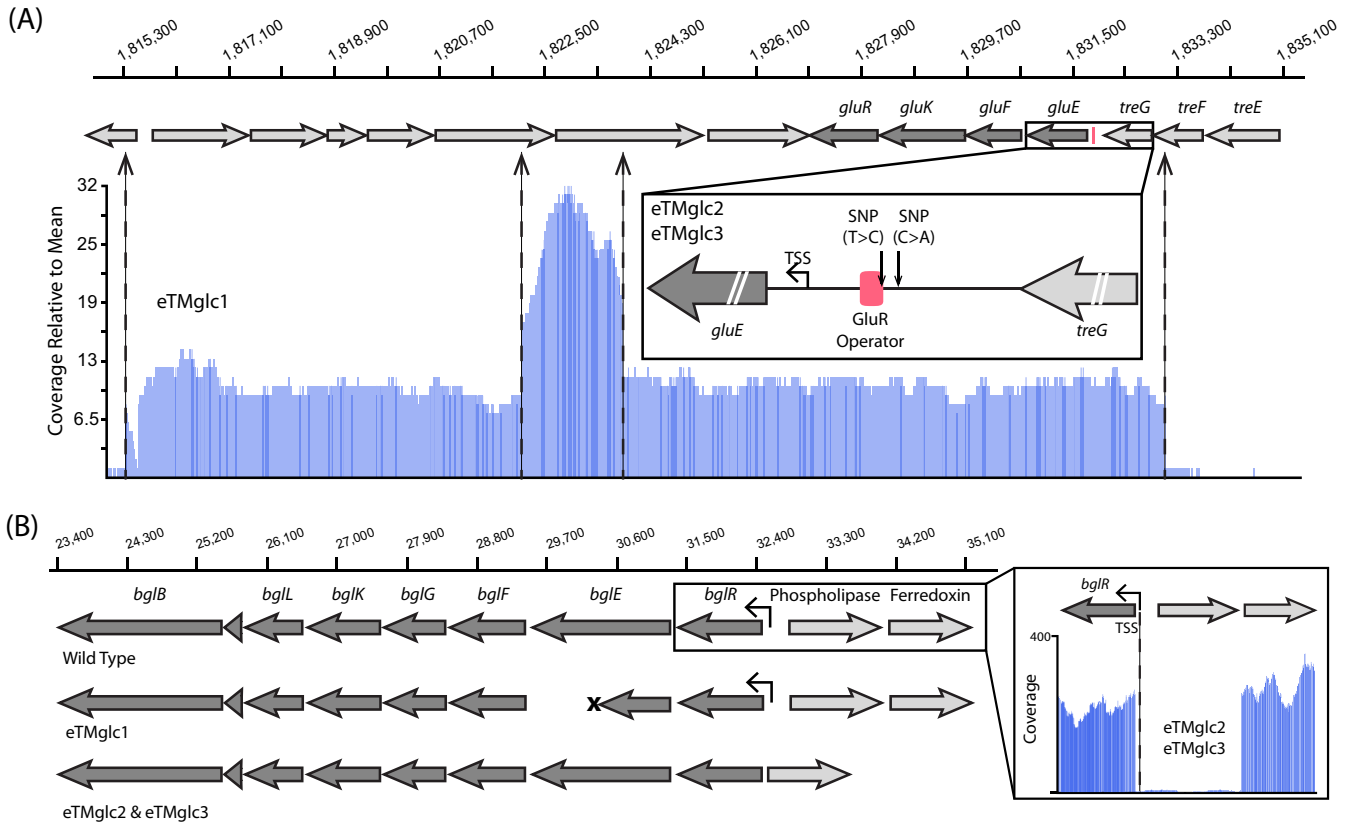

FIG 2 Mutations to the *gluEFK* and *bglEFGKL* ABC transporter operons. (A) Coverage is shown relative to the mean coverage across the entire genome for the genes spanning Tmari_1847 and Tmari_1861 to illustrate the gene duplication-amplification event observed in eTMglc1. The inset magnifies the intergenic region upstream of *gluE* to illustrate the positions of the point mutations relative to the GluR operator sequence (red) found in eTMglc2 and eTMglc3. The *gluEFK-gluR* operon is highlighted in dark gray. (B) Genes Tmari_0020 to Tmari_0031 are shown for the TM-wt, eTMglc1, and eTMglc2 and eTMglc3 (from top to bottom). The *bglEFGKL-bglR* genes are highlighted in dark gray. A nonsense mutation resulting in a truncated *bglE* gene is shown for eTMglc1. eTMglc2 and eTMglc3 carry a deletion that spans the intergenic regions upstream of *bglR* and ferredoxin and eliminates Tmari_0030 (inset).

the tmRNA secondary structure is likely to be unaffected by the deletion by compensatory base pairing with the G stretch.

Mutations were examined for potential impact on glucose metabolism. It is known that glucose is an effector for three locally acting transcription factors, i.e., GluR, BglR, and XylR (33, 34). The operons carrying *gluR* (Tmari_1855) and *bglR* (Tmari_0029) are found to have mutations in all three evolved replicate cultures. For eTMglc1, the entire glucose ABC transporter cassette (*gluEFK*, Tmari_1858 to Tmari_1856) and *gluR* are contained within a large gene duplication-amplification mutation that spans 17.8 kb from Tmari_1847 to Tmari_1860 (Fig. 2A). Genes in this region have a copy number estimated at 11×, with the exceptions of Tmari_1852 (maltodextrin glucosidase) and Tmari_1853 (pullulanase), which have a copy number of around 27×. eTMglc1 also has a nonsense mutation in the sugar binding protein gene, *bglE* (Tmari_0028), of the *bglEFGKL* (Tmari_0028 to Tmari-0024) ABC transporter (Fig. 2B). This transporter recognizes and imports beta-glucosides such as cellobiose. However, this mutation to *bglE* is near the center of the gene and eliminates key tryptophan residues (W381, W384, and W536) responsible for forming van der Waals interactions with cellobiose (53).

Similarly, eTMglc2 and eTMglc3 carry mutations associated with the *gluEFK* and *bglEFGKL* ABC transporter operons. These strains carry two point mutations in the intergenic region upstream of the solute binding protein of the *gluEFK* transporter (Tmari_1858, *gluE*). One of these mutations occurs in the GluR operator sequence, and the second is slightly upstream of the operator (Fig. 2A, inset). The *bglEFGKL* operon is directly affected by a large deletion that is upstream of the *bglR* gene; it spans Tmari_0030 and ends upstream of Tmari_0031, a gene coding for a ferredoxin (Fig. 2B). This mutation retains only four base pairs upstream of *bglR*, thereby eliminating the native promoter region and transcription start site of the *bglEFGKL* operon.

Gene expression analysis of eTMglc mutant cultures. To examine the potential impact of genetic mutations on gene expression, RNA-seq libraries were constructed from samples collected at mid-log phase during growth experiments performed in bioreactors. Data were generated for the three evolved replicates and compared to those for the wild type using the Cuffdiff package (40). A hypergeometric enrichment for significantly overrepresented clusters of orthologous groups (COGs) showed that only the carbohydrate transport and metabolism category (G) was significantly enriched in all three evolved cultures ($P < 0.05$) (see Fig. S2 in the supplemental material). This result prompted us to further examine the sugar regulons defined for *T. maritima* (33, 34). Hypergeometric enrichment of the sugar regulons (Fig. 3A) shows that genes regulated by GluR, BglR, AraR, IolR, and UgpR are overrepresented among the differentially expressed genes in all

(A)

eTMglc1	eTMglc2	eTMglc3	
8.8e−04	6.6e−04	4.3e−05	TreR
5.1e−04	3.4e−04	8.6e−04	AraR
4.6e−04	1.5e−05	7.3e−03	GluR
3.7e−06	2.4e−06	6.5e−06	IolR
1.6e−02	3.1e−07	1.2e−06	BglR
1.8e−02	2.0e−01	3.3e−05	XylR
2.6e−02	6.0e−01	9.6e−05	KdgR
3.4e−01	9.6e−03	4.3e−05	UctR
2.2e−02	1.8e−02	3.5e−03	UgpR
5.4e−01	2.5e−01	1.6e−01	UxaR
7.3e−01	2.4e−01	3.5e−01	CelR
2.4e−01	5.2e−01	2.8e−01	GloR
3.3e−01	3.0e−01	3.8e−01	ManR
6.8e−01	NaN	1.9e−01	RbsR
7.4e−01	NaN	NaN	RhaR
NaN	NaN	NaN	ChiR
5.3e−02	4.8e−01	6.8e−02	UgtR
3.0e−02	2.2e−01	3.0e−01	GalR

(B)

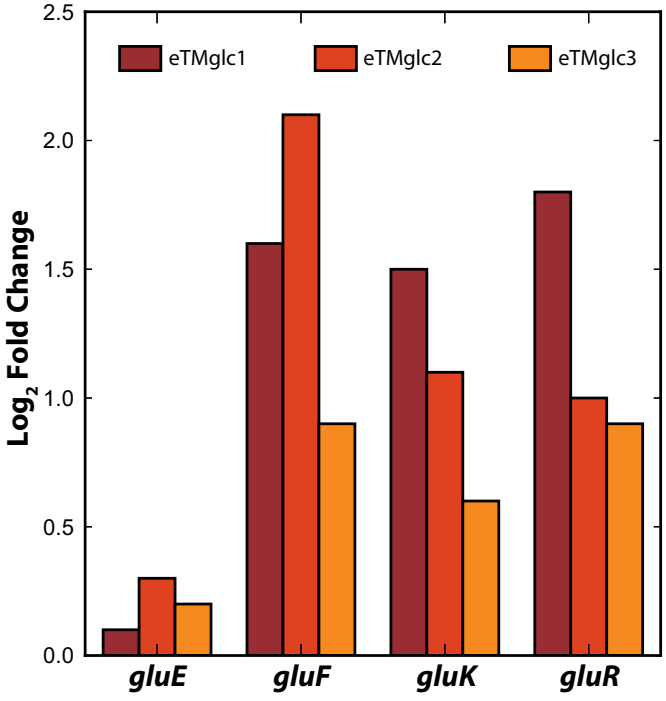

(C)

Locus Tag	Product	TM wt FPKM	eTMglc1 FPKM	eTMglc1 Log_2 Fold Change	eTMglc2 FPKM	eTMglc2 Log_2 Fold Change	eTMglc3 FPKM	eTMglc3 Log_2 Fold Change
Tmari_0029	*bglR*	1687	1429	0.36	44	-8.85	50	-6.44
Tmari_0028	*bglE*	**57875**	1262	-1.98	35	-9.12	40	-8.07
Tmari_0027	*bglF*	3476	619	-1.14	20	-8.25	30	-7.21
Tmari_0026	*bglG*	2722	981	-1.23	19	-7.90	33	-7.10
Tmari_0025	*bglK*	2255	1182	-0.93	14	-7.29	28	-6.32
Tmari_0024	*bglL*	2271	1163	-1.21	11	-6.87	20	-6.10
Tmari_0023	Tmari_0023	1419	1575	-1.20	11	-6.15	23	-5.58
Tmari_0022	Beta-glucosidase	2731	14621	-1.11	104	-6.28	215	-6.09
Tmari_0021	Laminarinase	4753	2171	-1.73	4	-6.76	19	-6.57

(D)

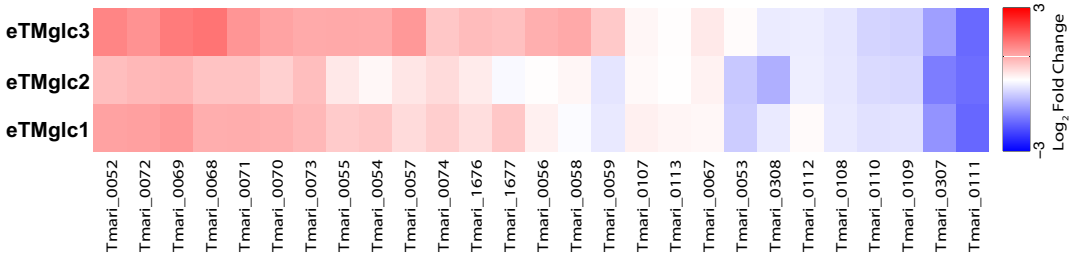

FIG 3 Gene expression analysis of eTMglc cultures. (A) Heat map illustrating the significance of the hypergeometric enrichment test performed on sugar regulons. Values in the blocks of the heat map correspond to their respective *P* values. (B) Increased gene expression of the *gluEFK* and *gluR* regulon in eTMglc cultures compared with wild type. Bars represent log_2 fold change for each gene in the operon. (C) Downregulation of the *bglEFGKL* operon for the eTMglc cultures. For each evolved culture, the FPKM value for each gene is shown as the log_2 fold change with respect to wild-type *T. maritima* grown on glucose. (D) Heat map of the log_2 fold change for the XylR regulon.

three evolved cultures, whereas the XylR, KdgR, TreR, GalR, and UctR regulons are enriched in only one or two of the evolved cultures.

Of the enriched regulons, GluR and BglR are of particular interest because of the presence of mutations that involve glucose transport and metabolism pathways. For GluR, there is upregulation of the *gluEFK* ABC transporter genes and *gluR* (Fig. 3B), whereas the BglR regulon is dramatically downregulated (Fig. 3C).

The first gene in the *gluEFK* operon, *gluE*, is not differentially expressed, but the subsequent genes are upregulated. *gluE* has the highest FPKM (a measure of transcript abundance) in the operon, as is common for solute binding proteins (54–56), and has a predicted secondary structure in the intergenic region between *gluE* and *gluF* that could be a target for posttranscriptional regulation (see Fig. S3 in the supplemental material). Expression of the *bglEFGKL* ABC transporter genes is nearly abolished in eTMglc2 and eTMglc3 where the upstream promoter is deleted. Similarly, the *bglE* gene carrying the nonsense mutation in eTMglc1 and all downstream genes are downregulated, with *bglE* having the largest fold change (1.98 $\log_2$). Glucose is a potential effector for XylR in *T. maritima*. Wild-type XylR is activated *in vitro* in the presence of glucose (33) but uninduced *in vivo* (34). XylR-regulated genes are predominantly upregulated in eTMglc1 and eTMglc3 (Fig. 3D). The enrichment of the KdgR regulon is likely due to fact that XylR and KdgR regulate many of the same genes. The three genes regulated solely by KdgR, Tmari_0060 to Tmari_0062, are not differentially expressed, further supporting XylR as the transcription factor causing upregulation in the evolved cultures.

Many of the *T. maritima* sugar regulons regulate genes encoding transporters belonging to the ABC2 uptake family (43, 45). TransporterTP predicts that *T. maritima* carries 139 genes whose products fall into 14 different ABC2 uptake families, with the two carbohydrate uptake transporter families (3.A.1.1 and 3.A.1.2) and the peptide/opine/nickel uptake transporter family (3.A.1.5) accounting for 107 (77%) of these genes. Of these 107 genes, 38, 33, and 39 were differentially expressed for eTMglc1, eTMglc2, and eTMglc3, respectively, representing 13 to 14% of all differentially expressed genes. Genes in these categories were characterized based on their predicted function using the categorization provided by ABCdb (57). This divided the cohort into three groups: solute binding proteins (S), proteins with membrane spanning-domains (M), and proteins with nucleotide binding domains that hydrolyze ATP to ADP (N). Genes from these categories for a given ABC transporter are often operonic and expressed in a single transcription unit (55, 58, 59).

Comparison of the absolute transcript levels (FPKMs) between genes in these categories showed that the levels for the solute binding proteins are higher than those observed for the membrane-spanning and ATP-hydrolyzing groups (Fig. 4A). However, examination of the evolved strains revealed a drop in the global FPKM distribution for the solute binding proteins. Differential expression analysis of the evolved strains relative to the wild-type strain confirmed that the global drop in the solute binding proteins is significantly greater than those for other constituents of ABC transporters (Fig. 4B). To examine this further, RNA-seq was performed on three independently adapted cultures on glycerol (see Tables S3, S4, and S5 in the supplemental material for growth physiology, gene expression of the proposed glycerol utilization genes, and genetic changes detected in glycerol-adapted cultures). Unlike most carbon sources, glycerol is proposed to enter *T. maritima* through facilitated diffusion rather than through ABC-mediated transport (20, 60). Therefore, when grown on glycerol, *T. maritima* does not benefit from overexpressing ABC importer genes. Analogous to the trends seen with the evolved cultures on glucose, the solute binding proteins had the highest expression levels but were relatively more downregulated in comparison with the wild-type strain (see Fig. S4 in the supplemental material). This indicates that the evolution on glucose results in a global regulatory response that streamlines the transcript levels of ABC2 uptake transporters and that this streamlining is achieved primarily by modulating the solute binding protein transcript levels.

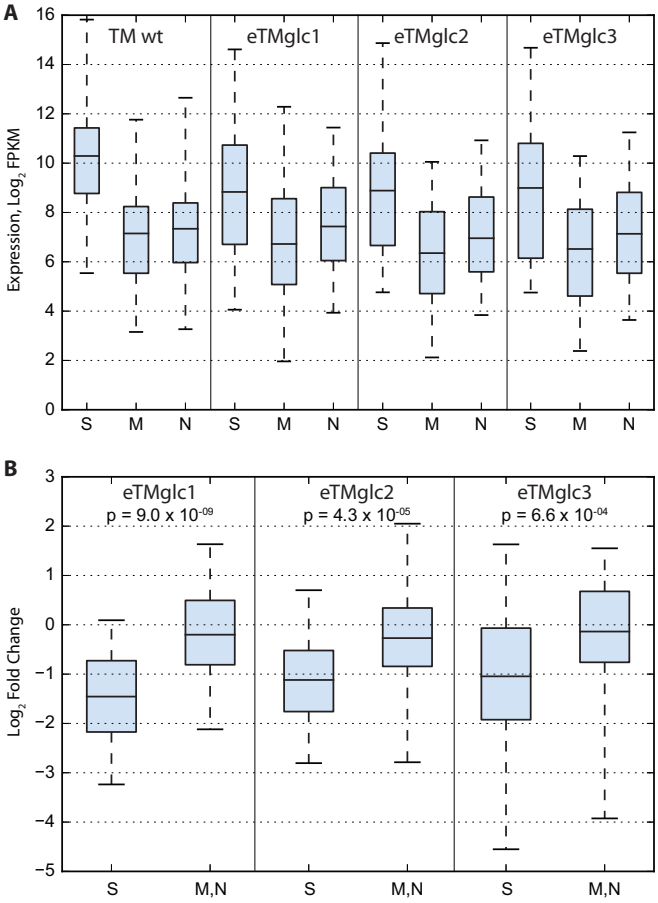

FIG 4 Gene expression analysis of the different functional categories of proteins found in the ABC2 importer families for carbohydrate uptake (3.A.1.1 and 3.A.1.2) and the peptide/opine/nickel uptake family (3.A.1.5) for cultures grown on glucose. (A) Box plots showing the absolute transcript abundance measures (FPKMs) for the different ABC transporter protein components across all cell lines. (B) Box plots showing the distribution of the $\log_2$ fold change for the different ABC transporter protein components for all evolved cell lines relative to wild type. The box plots show values falling within 95% confidence intervals, with the box comprising the interquartile range and the horizontal line within the box representing the mean. Two-tailed *P* values were determined using the Student *t* test. ABC transporter proteins are categorized as S for solute binding protein, M for membrane-spanning domain, and N for ATP-hydrolyzing protein.

DISCUSSION

Through the application of adaptive laboratory evolution, physiological characterization of evolved cultures, and an integrated multiomic characterization of evolved cultures, we are able to provide novel insights into the metabolic bottleneck in glucose metabolism for *T. maritima*. This study shows a clear connection between genomic changes and subsequent changes in transcription, which may ultimately explain the observed phenotype. Our findings suggest that *T. maritima* is capable of overcoming deficiencies in glucose metabolism in relatively short time frames. This organism achieved an enhanced phenotype within 25 days of the study onset with a CCD that is 1,000 times lower than that

typically observed in *E. coli* (51). The strains with the eTMglc phenotypes are capable of growing twice as fast as the wild type and utilize upwards of 57% more glucose. The rapid evolution and the vastly improved phenotype achieved on glucose suggest that the thermolability of glucose is unlikely to be the root cause for the poor growth achieved by *T. maritima* as has been previously suggested (29). Such a biophysical limitation in the sole carbon source would present a formidable challenge for the cells to overcome. Therefore, the poor growth on glucose is likely an inherent limitation in glucose uptake and metabolism.

This inherent limitation is further supported by the multiomic characterization of the genome and transcriptome and *in silico* analysis of the evolved cultures. In all evolved cultures, the genes regulated in the GluR and BglR regulons are also associated with genetic mutations. These locally acting transcription factors directly bind glucose as effectors (33, 34) and regulate operons encoding ABC2 uptake transporters. In the case of GluR, the gene expression of the glucose ABC transporter GluEFK was enhanced. The *gluEFK-gluR* operon was observed to undergo point mutations in the intergenic region upstream of *gluE*, one of which directly impacts the GluR operator sequence in two evolved cultures. The third culture was found to have repetitively undergone a gene amplification event that increased the gene dosage of the *gluEFK-gluR* operon. Interestingly, *gluEFK* and *treEFG* were only recently discovered in *T. maritima* after an initial omission of an ~10-kb region in the reference genome (32). In fact, the large duplication events discussed here span the entire ~10-kb region. It is thought that this region was omitted from the original genome assembly as a result of a deletion event that occurred during early subculturing (32). Furthermore, the most upstream gene of this duplication event, Tmari_1847, is part of one of two maltose ABC transporters in *T. maritima* that are thought to have arisen via a duplication event (21). Therefore, this segment of the genome appears to be rather unstable. Further characterization of this region may provide valuable insights into the evolutionary trajectory of ABC transporters.

Unlike the case for the GluEFK transporter, the evolved glucose strains substantially downregulate the *bglEFGKL* operon. *bglE*, the solute binding component, is the second most detected transcript in the wild-type culture, with a $\log_2$ FPKM of 15.8, but this is reduced to nearly zero in two of the evolved glucose cultures. This is the result of a chromosomal gene deletion to Tmari_0030, but, more importantly, the promoter governing expression of the operon carrying *bglEFGKL*, *bglR*, and other pathway genes is also eliminated. The third evolved culture harbors a nonsense mutation that truncates key amino acids necessary for binding of beta-glucosides (53). These changes to the functionality of BglEFGKL reveal a potential regulatory inefficiency due to effector overlap between GluR and BglR. Glucose induces a strong transcriptional response for *bglEFGKL*, which is known to transport only beta-glucoside polymers comprised of 2 to 5 monomers (53, 54, 61). Therefore, while GluR senses glucose and induces a beneficial transcriptional response, BglR activation by glucose produces a greater transcriptional response that is ineffectual in the uptake of glucose monomers. Consequently, cellular resources are diverted from producing more of the appropriate transport complex, GluEFK, to the transcription and translation of BglEFGKL ABC transporter complexes. This results in a growth disadvantage in the wild type compared with the glucose-evolved cultures. Ideally, these genetic changes would be introduced into the wild-type strain to verify the impact on the observed phenotype. However, *T. maritima* suffers from a lack of robust genetic manipulation tools needed to make this connection. Nevertheless, these mutational effects are reflected in the changes in the transcriptome described here. This provides strong evidence that these key mutations to the glucose-responsive ABC transporters contribute to the observed phenotype.

Furthermore, interrogating the global transcriptional response of ABC2 uptake porters revealed a global modulation of the transcript levels of the solute binding domain component in response to glucose evolution. The transcript abundance for the solute binding protein is greater than that found for the membrane-spanning domains and ATP-hydrolyzing proteins. This pattern of transcript abundance has been observed previously in ABC transporters (54–56), and it is thought to be due to a stabilizing hairpin in the intergenic region downstream of the solute binding protein that hinders 3′-5′ exonuclease activity (55, 58, 59). It has been demonstrated that elimination of the stabilizing hairpin of the solute binding protein greatly reduces transcript abundance in the *E. coli malEFG* operon and the *Bacillus subtilis pst* operon (55, 58, 59). In fact, all of the *T. maritima* solute binding proteins in the ABC2 uptake families for carbohydrate and peptide transport contain a predicted hairpin structure (see Fig. S5 in the supplemental material). Therefore, the higher transcript abundance for the solute binding protein genes is likely due to increased mRNA half-lives, and one would subsequently expect reduced fluctuations in the abundance measures for these highly stable transcripts. Yet, the strains evolved on glucose demonstrate greater downregulation of these genes than of the other components of ABC2 uptake porters. A similar observation was made for cultures adapted to grow on glycerol, a carbon source transported independent of ABC transporters. While the absolute transcript levels of the solute binding protein are high, they are lower in the evolved cultures than in the wild type, and the other ABC import complex proteins are relatively unchanged.

Overall, the evolved cultures appear to primarily modulate the transcript abundance of the solute binding proteins within the ABC2 uptake transporter network to achieve a more efficient phenotype streamlined for glucose utilization and metabolism. The evolved cultures expend less energy on expressing solute binding proteins that recognize unavailable carbon sources and focus more on increasing uptake of glucose. This drastic change in the solute binding protein transcript levels is not observed in the membrane-spanning or ATP-hydrolyzing components. Energetically, this potentially yields substantial savings, since the solute binding proteins are found in greater abundance than the other components of ABC transporters (55, 59). For instance, it has been estimated that the *E. coli* MalE is found at 20 to 40 times higher levels than MalF or MalK (55, 62–64). Furthermore, posttranscriptional control modulating the mRNA-stabilizing hairpin downstream of the solute binding protein cannot be ruled out. This method of regulation better explains the observation that the solute binding protein is downregulated while maintaining comparable levels of membrane-spanning and ATP-hydrolyzing components. Implementing a posttranscriptional mechanism that has limited impact on the membrane-spanning and ATP-hydrolyzing transcript abundance could also result in a faster response to a change in carbon source. The execution of additional laboratory evolution experiments on different carbon sources will help further unravel the regulatory mechanisms that govern the ABC

transporter network and lead to deeper insights into the evolutionary trajectory of this ubiquitous class of proteins.

ACKNOWLEDGMENTS

Funding for this work was provided by the Office of Science of the U.S. Department of Energy (DOE) under grants DE-FG02-08ER64686 and DE-FG02-09ER25917. H.L. is supported through the National Science Foundation Graduate Research Fellowship under grant DGE1144086.

REFERENCES

1. **Lynch M, Conery JS.** 2003. The origins of genome complexity. Science **302:**1401–1404. http://dx.doi.org/10.1126/science.1089370.
2. **Lynch M.** 2006. Streamlining and simplification of microbial genome architecture. Annu Rev Microbiol **60:**327–349. http://dx.doi.org/10.1146/annurev.micro.60.080805.142300.
3. **Andersson DI, Hughes D.** 2009. Gene amplification and adaptive evolution in bacteria. Annu Rev Genet **43:**167–195. http://dx.doi.org/10.1146/annurev-genet-102108-134805.
4. **Barrick JE, Yu DS, Yoon SH, Jeong H, Oh TK, Schneider D, Lenski RE, Kim JF.** 2009. Genome evolution and adaptation in a long-term experiment with *Escherichia coli*. Nature **461:**1243–1247. http://dx.doi.org/10.1038/nature08480.
5. **Janga SC, Collado-Vides J.** 2007. Structure and evolution of gene regulatory networks in microbial genomes. Res Microbiol **158:**787–794. http://dx.doi.org/10.1016/j.resmic.2007.09.001.
6. **Konstantinidis KT, Tiedje JM.** 2004. Trends between gene content and genome size in prokaryotic species with larger genomes. Proc Natl Acad Sci U S A **101:**3160–3165. http://dx.doi.org/10.1073/pnas.0308653100.
7. **McAdams HH, Srinivasan B, Arkin AP.** 2004. The evolution of genetic regulatory systems in bacteria. Nat Rev Genet **5:**169–178. http://dx.doi.org/10.1038/nrg1292.
8. **van Nimwegen E.** 2003. Scaling laws in the functional content of genomes. Trends Genet **19:**479–484. http://dx.doi.org/10.1016/S0168-9525(03)00203-8.
9. **Via S, Lande R.** 1985. Genotype-environment interaction and the evolution of phenotypic plasticity. Evolution **39:**505–522. http://dx.doi.org/10.2307/2408649.
10. **Koonin EV, Wolf YI.** 2010. Constraints and plasticity in genome and molecular-phenome evolution. Nat Rev Genet **11:**487–498. http://dx.doi.org/10.1038/nrg2810.
11. **Portnoy VA, Bezdan D, Zengler K.** 2011. Adaptive laboratory evolution—harnessing the power of biology for metabolic engineering. Curr Opin Biotechnol **22:**590–594. http://dx.doi.org/10.1016/j.copbio.2011.03.007.
12. **Conrad TM, Lewis NE, Palsson BO.** 2011. Microbial laboratory evolution in the era of genome-scale science. Mol Syst Biol **7:**509. http://dx.doi.org/10.1038/msb.2011.42.
13. **Hindre T, Knibbe C, Beslon G, Schneider D.** 2012. New insights into bacterial adaptation through *in vivo* and *in silico* experimental evolution. Nat Rev Microbiol **10:**352–365. http://dx.doi.org/10.1038/nrmicro2750.
14. **Goodarzi H, Bennett BD, Amini S, Reaves ML, Hottes AK, Rabinowitz JD, Tavazoie S.** 2010. Regulatory and metabolic rewiring during laboratory evolution of ethanol tolerance in *E. coli*. Mol Syst Biol **6:**378. http://dx.doi.org/10.1038/msb.2010.33.
15. **Sandberg TE, Pedersen M, LaCroix RA, Ebrahim A, Bonde M, Herrgard MJ, Palsson BO, Sommer M, Feist AM.** 2014. Evolution of *Escherichia coli* to 42° C and subsequent genetic engineering reveals adaptive mechanisms and novel mutations. Mol Biol Evol **31:**2647–2662. http://dx.doi.org/10.1093/molbev/msu209.
16. **Lee DH, Palsson BO.** 2010. Adaptive evolution of *Escherichia coli* K-12 MG1655 during growth on a nonnative carbon source, L-1,2-propanediol. Appl Environ Microbiol **76:**4158–4168. http://dx.doi.org/10.1128/AEM.00373-10.
17. **Munoz R, Yarza P, Ludwig W, Euzeby J, Amann R, Schleifer KH, Glockner FO, Rossello-Mora R.** 2011. Release LTPs104 of the All-Species Living Tree. Syst Appl Microbiol **34:**169–170. http://dx.doi.org/10.1016/j.syapm.2011.03.001.
18. **Achenbach-Richter L, Gupta R, Stetter KO, Woese CR.** 1987. Were the original eubacteria thermophiles? Syst Appl Microbiol **9:**34–39. http://dx.doi.org/10.1016/S0723-2020(87)80053-X.
19. **Zhaxybayeva O, Swithers KS, Lapierre P, Fournier GP, Bickhart DM, DeBoy RT, Nelson KE, Nesbo CL, Doolittle WF, Gogarten JP, Noll KM.** 2009. On the chimeric nature, thermophilic origin, and phylogenetic placement of the Thermotogales. Proc Natl Acad Sci U S A **106:**5865–5870. http://dx.doi.org/10.1073/pnas.0901260106.
20. **Nelson KE, Clayton RA, Gill SR, Gwinn ML, Dodson RJ, Haft DH, Hickey EK, Peterson JD, Nelson WC, Ketchum KA, McDonald L, Utterback TR, Malek JA, Linher KD, Garrett MM, Stewart AM, Cotton MD, Pratt MS, Phillips CA, Richardson D, Heidelberg J, Sutton GG, Fleischmann RD, Eisen JA, White O, Salzberg SL, Smith HO, Venter JC, Fraser CM.** 1999. Evidence for lateral gene transfer between Archaea and Bacteria from genome sequence of *Thermotoga maritima*. Nature **399:**323–329. http://dx.doi.org/10.1038/20601.
21. **Noll KM, Lapierre P, Gogarten JP, Nanavati DM.** 2008. Evolution of mal ABC transporter operons in the Thermococcales and Thermotogales. BMC Evol Biol **8:**7. http://dx.doi.org/10.1186/1471-2148-8-7.
22. **Nesbo CL, Dlutek M, Doolittle WF.** 2006. Recombination in Thermotoga: implications for species concepts and biogeography. Genetics **172:**759–769.
23. **Mongodin EF, Hance IR, Deboy RT, Gill SR, Daugherty S, Huber R, Fraser CM, Stetter K, Nelson KE.** 2005. Gene transfer and genome plasticity in *Thermotoga maritima*, a model hyperthermophilic species. J Bacteriol **187:**4935–4944. http://dx.doi.org/10.1128/JB.187.14.4935-4944.2005.
24. **Ben Hania W, Postec A, Aullo T, Ranchou-Peyruse A, Erauso G, Brochier-Armanet C, Hamdi M, Ollivier B, Saint-Laurent S, Magot M, Fardeau ML.** 2013. *Mesotoga infera* sp. nov., a mesophilic member of the order *Thermotogales*, isolated from an underground gas storage aquifer. Int J Syst Evol Microbiol **63:**3003–3008. http://dx.doi.org/10.1099/ijs.0.047993-0.
25. **Nesbo CL, Doolittle WF.** 2003. Targeting clusters of transferred genes in *Thermotoga maritima*. Environ Microbiol **5:**1144–1154. http://dx.doi.org/10.1046/j.1462-2920.2003.00515.x.
26. **Nesbo CL, L'Haridon S, Stetter KO, Doolittle WF.** 2001. Phylogenetic analyses of two "archaeal" genes in *Thermotoga maritima* reveal multiple transfers between archaea and bacteria. Mol Biol Evol **18:**362–375. http://dx.doi.org/10.1093/oxfordjournals.molbev.a003812.
27. **Martin W, Baross J, Kelley D, Russell MJ.** 2008. Hydrothermal vents and the origin of life. Nat Rev Microbiol **6:**805–814. http://dx.doi.org/10.1038/nrmicro1991.
28. **Huber R, Langworthy T, König H, Thomm M, Woese C, Sleytr U, Stetter K.** 1986. *Thermotoga maritima* sp. nov. represents a new genus of unique extremely thermophilic eubacteria growing up to 90°C. Arch Microbiol **144:**324–333.
29. **Conners SB, Mongodin EF, Johnson MR, Montero CI, Nelson KE, Kelly RM.** 2006. Microbial biochemistry, physiology, and biotechnology of hyperthermophilic *Thermotoga* species. FEMS Microbiol Rev **30:**872–905. http://dx.doi.org/10.1111/j.1574-6976.2006.00039.x.
30. **Frock AD, Notey JS, Kelly RM.** 2010. The genus *Thermotoga*: recent developments. Environ Technol **31:**1169–1181. http://dx.doi.org/10.1080/09593330.2010.484076.
31. **Latif H, Lerman JA, Portnoy VA, Tarasova Y, Nagarajan H, Schrimpe-Rutledge AC, Smith RD, Adkins JN, Lee DH, Qiu Y, Zengler K.** 2013. The genome organization of *Thermotoga maritima* reflects its lifestyle. PLoS Genet **9:**e1003485. http://dx.doi.org/10.1371/journal.pgen.1003485.
32. **Boucher N, Noll KM.** 2011. Ligands of thermophilic ABC transporters encoded in a newly sequenced genomic region of *Thermotoga maritima* MSB8 screened by differential scanning fluorimetry. Appl Environ Microbiol **77:**6395–6399. http://dx.doi.org/10.1128/AEM.05418-11.
33. **Kazanov MD, Li X, Gelfand MS, Osterman AL, Rodionov DA.** 2013. Functional diversification of ROK-family transcriptional regulators of sugar catabolism in the Thermotogae phylum. Nucleic Acids Res **41:**790–803. http://dx.doi.org/10.1093/nar/gks1184.
34. **Rodionov DA, Rodionova IA, Li X, Ravcheev DA, Tarasova Y, Portnoy VA, Zengler K, Osterman AL.** 2013. Transcriptional regulation of the carbohydrate utilization network in *Thermotoga maritima*. Front Microbiol **4:**244. http://dx.doi.org/10.3389/fmicb.2013.00244.
35. **Chhabra SR, Shockley KR, Conners SB, Scott KL, Wolfinger RD, Kelly RM.** 2003. Carbohydrate-induced differential gene expression patterns in the hyperthermophilic bacterium *Thermotoga maritima*. J Biol Chem **278:**7540–7552. http://dx.doi.org/10.1074/jbc.M211748200.
36. **Frock AD, Gray SR, Kelly RM.** 2012. Hyperthermophilic *Thermotoga* species differ with respect to specific carbohydrate transporters and glyco-

side hydrolases. Appl Environ Microbiol **78:**1978–1986. http://dx.doi.org/10.1128/AEM.07069-11.
37. **Rinker KD, Kelly RM.** 1996. Growth physiology of the hyperthermophilic archaeon *Thermococcus litoralis*: development of a sulfur-free defined medium, characterization of an exopolysaccharide, and evidence of biofilm formation. Appl Environ Microbiol **62:**4478–4485.
38. **Levin JZ, Yassour M, Adiconis X, Nusbaum C, Thompson DA, Friedman N, Gnirke A, Regev A.** 2010. Comprehensive comparative analysis of strand-specific RNA sequencing methods. Nat Methods **7:**709–715. http://dx.doi.org/10.1038/nmeth.1491.
39. **Langmead B, Salzberg SL.** 2012. Fast gapped-read alignment with Bowtie 2. Nat Methods **9:**357–359. http://dx.doi.org/10.1038/nmeth.1923.
40. **Trapnell C, Hendrickson DG, Sauvageau M, Goff L, Rinn JL, Pachter L.** 2013. Differential analysis of gene regulation at transcript resolution with RNA-seq. Nat Biotechnol **31:**46–53. http://dx.doi.org/10.1038/nbt.2450.
41. **Novichkov PS, Kazakov AE, Ravcheev DA, Leyn SA, Kovaleva GY, Sutormin RA, Kazanov MD, Riehl W, Arkin AP, Dubchak I, Rodionov DA.** 2013. RegPrecise 3.0—a resource for genome-scale exploration of transcriptional regulation in bacteria. BMC Genomics **14:**745. http://dx.doi.org/10.1186/1471-2164-14-745.
42. **Markowitz VM, Chen IM, Palaniappan K, Chu K, Szeto E, Grechkin Y, Ratner A, Jacob B, Huang J, Williams P, Huntemann M, Anderson I, Mavromatis K, Ivanova NN, Kyrpides NC.** 2012. IMG: the Integrated Microbial Genomes database and comparative analysis system. Nucleic Acids Res **40:**D115–D122. http://dx.doi.org/10.1093/nar/gkr1044.
43. **Saier MH, Jr, Reddy VS, Tamang DG, Vastermark A.** 2014. The transporter classification database. Nucleic Acids Res **42:**D251–D258. http://dx.doi.org/10.1093/nar/gkt1097.
44. **Li H, Benedito VA, Udvardi MK, Zhao PX.** 2009. TransportTP: a two-phase classification approach for membrane transporter prediction and characterization. BMC Bioinformatics **10:**418. http://dx.doi.org/10.1186/1471-2105-10-418.
45. **Zheng WH, Vastermark A, Shlykov MA, Reddy V, Sun EI, Saier MH, Jr.** 2013. Evolutionary relationships of ATP-binding cassette (ABC) uptake porters. BMC Microbiol **13:**98. http://dx.doi.org/10.1186/1471-2180-13-98.
46. **Lorenz R, Bernhart SH, Honer Zu Siederdissen C, Tafer H, Flamm C, Stadler PF, Hofacker IL.** 2011. ViennaRNA package 2.0. Algorithms Mol Biol **6:**26. http://dx.doi.org/10.1186/1748-7188-6-26.
47. **Nogales J, Gudmundsson S, Thiele I.** 2012. An *in silico* re-design of the metabolism in *Thermotoga maritima* for increased biohydrogen production. Int J Hydrogen Energy **37:**12205–12218. http://dx.doi.org/10.1016/j.ijhydene.2012.06.032.
48. **Schellenberger J, Palsson BO.** 2009. Use of randomized sampling for analysis of metabolic networks. J Biol Chem **284:**5457–5461. http://dx.doi.org/10.1074/jbc.R800048200.
49. **Bordbar A, Lewis NE, Schellenberger J, Palsson BO, Jamshidi N.** 2010. Insight into human alveolar macrophage and *M. tuberculosis* interactions via metabolic reconstructions. Mol Syst Biol **6:**422. http://dx.doi.org/10.1038/msb.2010.68.
50. **Schellenberger J, Que R, Fleming RM, Thiele I, Orth JD, Feist AM, Zielinski DC, Bordbar A, Lewis NE, Rahmanian S, Kang J, Hyduke DR, Palsson BO.** 2011. Quantitative prediction of cellular metabolism with constraint-based models: the COBRA Toolbox v2.0. Nat Protoc **6:**1290–1307. http://dx.doi.org/10.1038/nprot.2011.308.
51. **LaCroix RA, Sandberg TE, O'Brien EJ, Utrilla J, Ebrahim A, Guzman GI, Szubin R, Palsson BO, Feist AM.** 10 October 2014. Discovery of key mutations enabling rapid growth of *Escherichia coli* K-12 MG1655 on glucose minimal media using adaptive laboratory evolution. Appl Environ Microbiol http://dx.doi.org/10.1128/AEM.02246-14.
52. **Zwieb C, Gorodkin J, Knudsen B, Burks J, Wower J.** 2003. tmRDB (tmRNA database). Nucleic Acids Res **31:**446–447. http://dx.doi.org/10.1093/nar/gkg019.
53. **Cuneo MJ, Beese LS, Hellinga HW.** 2009. Structural analysis of semi-specific oligosaccharide recognition by a cellulose-binding protein of *Thermotoga maritima* reveals adaptations for functional diversification of the oligopeptide periplasmic binding protein fold. J Biol Chem **284:**33217–33223. http://dx.doi.org/10.1074/jbc.M109.041624.
54. **Nanavati DM, Nguyen TN, Noll KM.** 2005. Substrate specificities and expression patterns reflect the evolutionary divergence of maltose ABC transporters in *Thermotoga maritima*. J Bacteriol **187:**2002–2009. http://dx.doi.org/10.1128/JB.187.6.2002-2009.2005.
55. **Newbury SF, Smith NH, Higgins CF.** 1987. Differential mRNA stability controls relative gene expression within a polycistronic operon. Cell **51:**1131–1143. http://dx.doi.org/10.1016/0092-8674(87)90599-X.
56. **Stern MJ, Prossnitz E, Ames GF.** 1988. Role of the intercistronic region in post-transcriptional control of gene expression in the histidine transport operon of *Salmonella typhimurium*: involvement of REP sequences. Mol Microbiol **2:**141–152. http://dx.doi.org/10.1111/j.1365-2958.1988.tb00015.x.
57. **Fichant G, Basse MJ, Quentin Y.** 2006. ABCdb: an online resource for ABC transporter repertories from sequenced archaeal and bacterial genomes. FEMS Microbiol Lett **256:**333–339. http://dx.doi.org/10.1111/j.1574-6968.2006.00139.x.
58. **Allenby NE, O'Connor N, Pragai Z, Carter NM, Miethke M, Engelmann S, Hecker M, Wipat A, Ward AC, Harwood CR.** 2004. Post-transcriptional regulation of the *Bacillus subtilis pst* operon encoding a phosphate-specific ABC transporter. Microbiology **150:**2619–2628. http://dx.doi.org/10.1099/mic.0.27126-0.
59. **Newbury SF, Smith NH, Robinson EC, Hiles ID, Higgins CF.** 1987. Stabilization of translationally active mRNA by prokaryotic REP sequences. Cell **48:**297–310. http://dx.doi.org/10.1016/0092-8674(87)90433-8.
60. **Maru BT, Bielen AAM, Constantí M, Medina F, Kengen SWM.** 2013. Glycerol fermentation to hydrogen by *Thermotoga maritima*: proposed pathway and bioenergetic considerations. Int J Hydrogen Energy **38:**5563–5572. http://dx.doi.org/10.1016/j.ijhydene.2013.02.130.
61. **Conners SB, Montero CI, Comfort DA, Shockley KR, Johnson MR, Chhabra SR, Kelly RM.** 2005. An expression-driven approach to the prediction of carbohydrate transport and utilization regulons in the hyperthermophilic bacterium *Thermotoga maritima*. J Bacteriol **187:**7267–7282. http://dx.doi.org/10.1128/JB.187.21.7267-7282.2005.
62. **Koman A, Harayama S, Hazelbauer GL.** 1979. Relation of chemotactic response to the amount of receptor: evidence for different efficiencies of signal transduction. J Bacteriol **138:**739–747.
63. **Manson MD, Boos W, Bassford PJ, Jr, Rasmussen BA.** 1985. Dependence of maltose transport and chemotaxis on the amount of maltose-binding protein. J Biol Chem **260:**9727–9733.
64. **Shuman HA, Silhavy TJ, Beckwith JR.** 1980. Labeling of proteins with beta-galactosidase by gene fusion. Identification of a cytoplasmic membrane component of the *Escherichia coli* maltose transport system. J Biol Chem **255:**168–174.